Submitted to *Rheologica Acta*
to accompany the re-submission of Manuscript ID RA-09-05-0051 entitled "Large amplitude oscillatory shear of pseudoplastic and elastoviscoplastic materials"

On secondary loops in LAOS via self-intersection of Lissajous-Bowditch curves

Randy H. Ewoldt and Gareth H. McKinley*
Hatsopoulos Microfluids Laboratory, Department of Mechanical Engineering, Massachusetts Institute of Technology, Cambridge, MA

*author to whom correspondence should be addressed, gareth@mit.edu

Abstract

When the shear stress measured in Large Amplitude Oscillatory Shear (LAOS) deformation is represented as a two-dimensional Lissajous-Bowditch curve, the corresponding trajectory can appear to self-intersect and form secondary loops. This self-intersection is a general consequence of a strongly nonlinear material response to the imposed oscillatory forcing and can be observed for various material systems and constitutive models. We derive the mathematical criteria for the formation of secondary loops, quantify the location of the apparent intersection, and furthermore suggest a qualitative physical understanding for the associated nonlinear material behavior. We show that when secondary loops appear in the viscous projection of the stress response (the 2-D plot of stress vs. strain-rate) they are best interpreted by understanding the corresponding elastic response (the 2-D projection of stress vs. strain) The analysis shows clearly that sufficiently strong *elastic* nonlinearity is required to observe secondary loops on the conjugate *viscous* projection. Such a strong elastic nonlinearity physically corresponds to a nonlinear viscoelastic shear stress overshoot in which existing stress is unloaded more quickly than new deformation is accumulated. This general understanding of secondary loops in LAOS flows can be applied to various molecular configurations and microstructures such as polymer solutions, polymer melts, soft glassy materials and other structured fluids.

Keywords: Nonlinear viscoelasticity – Large Amplitude Oscillatory Shear (LAOS) – Lissajous-Bowditch curve – stress overshoot

Introduction

Large amplitude oscillatory shear (LAOS) is a class of flow that is commonly used to characterize nonlinear viscoelastic material responses (Giacomin and Dealy (1993)). In strain-controlled LAOS deformation, the imposed strain takes the form $\gamma(t) = \gamma_0 \sin \omega t$, which consequently subjects the sample to a corresponding oscillatory strain-rate, $\dot{\gamma} = \gamma_0 \omega \cos \omega t$. The steady state material stress response $\sigma(t; \gamma_0, \omega)$ oscillates with the same fundamental period as the imposed deformation, $T=2\pi/\omega$, but with a viscoelastic phase shift, as well as higher harmonic contributions when the imposed strain is high enough to induce material nonlinearity (Wilhelm (2002)).

LAOS responses can be visualized as parametric curves (properly termed Lissajous-Bowditch curves) of the oscillating stress $\sigma(t)$ vs. strain $\gamma(t)$, or stress $\sigma(t)$ vs. strain-rate $\dot{\gamma}(t)$. More generally this response can be represented in terms of closed space-curves within a 3-D coordinate system with strain $\gamma(t)$, strain-rate $\dot{\gamma}(t)$, and stress $\sigma(t)$ as the orthogonal coordinate axes (Fig. 1a). The 2-D Lissajous-Bowditch curves commonly represented in papers are then readily understood as projections of the fully 3-D coordinate space that describes the material response to oscillatory shearing. The 2-D projection onto the stress $\sigma(t)$ vs. strain $\gamma(t)$ plane views the material response from an elastic perspective (Fig. 1b), and a purely elastic material response would be a single-valued function of strain on this plane, $\sigma(\gamma)$. The viscous perspective is achieved by projecting the 3-D material trajectory onto the plane of stress $\sigma(t)$ vs. strain-rate $\dot{\gamma}(t)$ as shown in Fig. 1c. In this work we focus on the long-time steady-state oscillatory material response that is represented by a closed space-curve; however time-varying material responses associated with thixotropy, shear-induced migration or rheological aging etc. can also be represented in this material phase-space by trajectories that slowly decay towards the corresponding periodic attractor.

We are interested here in the self-intersection of Lissajous-Bowditch curves which form "secondary loops" (Fig. 1c, points I_1 and I_2), a visually-prominent phenomenon that quickly draws questions from the rheological observer. The interpretation of secondary loops has, to date, been limited to the study of specific material examples, being related to physical microstructural features such as non-affine deformation (Jeyaseelan and Giacomin (2008)) and

the absence of long-chain branching in polymer melts (Stadler *et al.* (2008)). However, such secondary loops have been observed for many different material systems including micellar solutions (Ewoldt *et al.* (2008)), a polystyrene solution (Jeyaseelan and Giacomin (2008)), several molten polymers (Tee and Dealy (1975), Stadler *et al.* (2008)), star-polymer networks (Rogers and Vlassopoulos (2009)), as well as Xanthan gum solutions and an invert-emulsion drilling fluid (see Ewoldt et al., Rheol Acta, accompanying manuscript). Nonlinear constitutive models can also show secondary loops, examples include a non-affine network model (Jeyaseelan and Giacomin (2008)), a tube-based model of entangled linear polymers (Leygue *et al.* (2006); Stadler *et al.* (2008)), and a single mode Giesekus model (demonstrated here). Owing to the variety of systems which show secondary loops, we seek to provide a general interpretation of this nonlinear rheological phenomenon.

The mathematical criteria for self-intersection of viscous Lissajous-Bowditch curves of stress $\sigma(t)$ vs. strain-rate $\dot{\gamma}(t)$ have been considered previously by Stadler *et al.* (2008) and Burhin *et al.* (2008), who have identified multiple criteria which must be simultaneously satisfied by the higher harmonic components of the stress response. Here we derive a criterion related to a *single* viscoelastic parameter which was recently proposed as a measure of nonlinear viscoelasticity, namely the minimum strain modulus $G'_M \equiv \left.\frac{d\sigma}{d\gamma}\right|_{\gamma=0} < 0$ (Ewoldt *et al.* (2008)). The criterion is understood through the connection between the 3-D Lissajous-Bowditch curves and the corresponding Chebyshev decomposition of the LAOS response. Furthermore, we address the theoretical possibility (unobserved to date) of self-intersection of the elastic projection of stress $\sigma(t)$ vs. strain $\gamma(t)$ and show, by analogy, that a single criterion, $\eta'_M < 0$, can be used to identify the conjugate phenomenon.

These mathematical criteria are related to viscoelastic parameters and therefore offer a general physical interpretation of the nonlinear material response associated with secondary loops.

Giesekus model example

A single-mode Giesekus model is used here as a canonical example in which secondary loops arise within a certain range of the Pipkin parameter space represented by frequency and strain

amplitude (ω, γ_0). The constitutive equation for the Giesekus model, as presented by Bird *et al.* (1987), is given by

$$\begin{aligned} &\boldsymbol{\sigma} = \boldsymbol{\sigma}_s + \boldsymbol{\sigma}_p \\ &\boldsymbol{\sigma}_s = \eta_s \dot{\boldsymbol{\gamma}} \\ &\boldsymbol{\sigma}_p + \lambda_1 \boldsymbol{\sigma}_{p(1)} + \alpha \frac{\lambda_1}{\eta_p} \{\boldsymbol{\sigma}_p \cdot \boldsymbol{\sigma}_p\} = \eta_p \dot{\boldsymbol{\gamma}}. \end{aligned} \tag{1}$$

Here $\boldsymbol{\sigma}_s$ is the solvent stress tensor, $\boldsymbol{\sigma}_p$ is the polymer stress tensor, $\boldsymbol{\sigma}_{p(1)}$ is the upper convected time derivative of the polymer stress, η_s is the solvent viscosity, η_p is the polymer viscosity, λ_1 is the relaxation time, and α is the mobility factor which gives rise to a nonlinear viscoelastic response (for $\alpha \neq 0$). The LAOS simulation is performed as described by Ewoldt *et al.* (2008) using the following model parameters, $\lambda_1 = 1$ s, $\eta_s = 0.01$ Pa.s, $\eta_p = 10$ Pa.s, and $\alpha = 0.3$. These four independent parameters result in a retardation time scale $\lambda_2 = \lambda_1 \eta_s / (\eta_s + \eta_p) = 0.001$ s and a polymeric shear modulus $G = \eta_p / \lambda_1 = 10$ Pa. A range of frequencies and strain amplitudes were simulated (Ewoldt *et al.* (2008)), $0.01 \leq \lambda_1 \omega \leq 1000$, $0.001 \leq \gamma_0 \leq 100$. Within this range, secondary loops were observed for a range of frequencies, $\lambda_1 \omega = 0.01 - 100$, at sufficiently large strain amplitude γ_0. Fig. 1 shows the steady state Lissajous-Bowditch curves associated with $\lambda_1 \omega = 1$, $\gamma_0 = 5.62$, for the single-mode Gieskus model, Eq. (1). Arrows are used to indicate the trajectory for each curve. Note that, in the absence of secondary loops, elastic curves are traversed in a clockwise direction (Fig. 1b) whereas the corresponding viscous curves propagate counterclockwise (Fig. 1c). The viscous projection onto the 2-D plane of stress $\sigma(t)$ and strain-rate $\dot{\gamma}(t)$ appears to intersect at points I_1 and I_2.

Criteria and interpretation of self-intersection

It is impossible for a fully 3-D Lissajous-Bowditch curve at steady state to intersect itself since the controlled input coordinates ($\gamma(t)$, $\dot{\gamma}(t)$) are orthogonal and always occupy unique values throughout a single cycle, i.e. the 2-D projection onto the plane of ($\gamma(t)$, $\dot{\gamma}(t)$) does not intersect. However, a 2-D projection onto the other coordinate planes of ($\sigma(t)$, $\gamma(t)$) or ($\sigma(t)$, $\dot{\gamma}(t)$) has the opportunity to self-intersect because the individual inputs of strain $\gamma(t)$ or strain-rate $\dot{\gamma}(t)$ take repeated values within a single period T=2π/ω. A sufficiently nonlinear

response may thus result in a 2-D response curve *projection* that intersects itself and forms secondary loops, such as those which appear in the curve of Fig. 1c.

To proceed with the quantitative criterion for self-intersection, we must introduce a mathematical representation of LAOS response curves. For an oscillatory strain input, $\gamma(t) = \gamma_0 \sin \omega t$, the viscoelastic stress response can be written as a time-domain Fourier series of odd-harmonics (Giacomin and Dealy (1993)),

$$\sigma\left(t;\omega,\gamma_0\right) = \gamma_0 \sum_{n:odd} \left\{ G_n'\left(\omega,\gamma_0\right) \sin n\omega t + G_n''\left(\omega,\gamma_0\right) \cos n\omega t \right\} \tag{2}$$

For sufficiently small strain amplitude γ_0, a linear material response is observed such that only the fundamental harmonic appears, $n = 1$ with a temporal phase shift δ_1 given by $\tan\delta_1 = G_1''/G_1'$. For larger deformation amplitudes, higher harmonics appear and the response is nonlinear. We argue that it is more meaningful to mathematically represent the measured material stress as a function of the time-varying kinematic inputs, strain $\gamma(t)$ and strain-rate $\dot{\gamma}(t)$, rather than time itself. This is consistent with the closed space-curve shown in Fig. 1c, $\sigma(\gamma(t),\dot{\gamma}(t))$. The stress response can be decomposed into a superposition of instantaneous elastic and viscous components (Cho *et al.* (2005)), which are single-valued functions of normalized strain $x(t) = \gamma(t)/\gamma_0$ and normalized strain-rate $y(t) = \dot{\gamma}(t)/\dot{\gamma}_0$ respectively. We write the superposition as $\sigma(t) = \sigma'(x(t)) + \sigma''(y(t))$. The decomposition into the elastic stress $\sigma'(x(t))$ and viscous stress $\sigma''(y(t))$ can then be written as a series of Chebyshev polynomials of the first kind (Ewoldt *et al.* (2008)),

$$\begin{aligned} \sigma'\left(x;\omega,\gamma_0\right) &= \gamma_0 \sum_n e_n\left(\omega,\gamma_0\right) T_n(x) \\ \sigma''\left(y;\omega,\gamma_0\right) &= \dot{\gamma}_0 \sum_n v_n\left(\omega,\gamma_0\right) T_n(y) \end{aligned} \tag{2}$$

in which the elastic and viscous coefficients, $e_n(\omega,\gamma_0)$ and $v_n(\omega,\gamma_0)$, have a physical interpretation and are directly related to the time-domain Fourier coefficients of Eq. (2) via $e_n = G_n'(-1)^{\frac{n-1}{2}}$ and $v_n = G_n''/\omega$ (n: odd).

The (apparent) intersection locations, I_1 and I_2 (Fig. 1), are defined by the criteria that the shear stress in the material takes repeated values at the same shear rate, but at different values of strain, $\sigma(\dot{\gamma},\gamma_1) = \sigma(\dot{\gamma},\gamma_2)$. This requires the total stress to be independent of the instantaneous

strain at I_1 and I_2, and therefore the elastic stress must be instantaneously zero at these points. Thus, self-intersection occurs when

$$\sigma'(x(t)) = 0, \quad x \neq 0 \tag{3}$$

where $x(t) = \gamma(t)/\gamma_0$. This can be visualized in Fig.1b which shows that the elastic stress is instantaneously zero, $\sigma'(\gamma(t)) = 0$, at the apparent intersection points I_1 and I_2. Correspondingly, Fig. 1c shows that the total stress is equal to the instantaneous viscous stress at points I_1 and I_2, $\sigma(t) = \sigma''(\dot{\gamma}(t))$.

An intersection of the *viscous* projection therefore occurs when the instantaneous value of the decomposed *elastic* stress passes through zero at a non-zero value of $x(t) = \gamma(t)/\gamma_0$. This intersection point can be located by expanding the elastic stress in terms of the Chebyshev polynomials of the first kind (Eq. (2)), $\sigma'(x) = \gamma_0 \left\{ e_1 x + e_3 (4x^3 - 3x) + ... \right\}$. The criteria that $\sigma'(x_I) = 0$ at points I_1 and I_2 results in the leading order non-zero solution that I_1 and I_2 occur at real values of

$$\begin{aligned} x_I &= \mp \frac{1}{2} \sqrt{3 - \left(\frac{e_1}{e_3} \right)} \\ y_I &= \cos\left[\sin^{-1}\left(x_I \right) \right]. \end{aligned} \tag{4}$$

Real values of x_I are achieved for $e_3/e_1 > 1/3$ (to leading order), i.e. the self-intersection of *viscous* curves results from sufficiently strong *elastic* non-linearity. The visually-dominant feature of the material nonlinearity thus appears as secondary loops on the *viscous* Lissajous-Bowditch curve, but it is best interpreted as a consequence of a nonlinear *elastic* phenomenon.

We now identify a single parameter which indicates the presence of self-intersection, rather than searching the decomposed stresses for zero-crossings. Consider the general criterion for self-intersection, Eq. (3), $\sigma'(x) = 0$ for $x \neq 0$, combined with the fact that the elastic stress $\sigma'(x)$ has odd-symmetry about $x = 0$ with a necessary zero-crossing at $x = 0$ (so that when $\gamma = 0$ we have an instantaneous elastic stress $\sigma' = 0$). Loops form when $\sigma'(x) = 0$ at locations other than $x = 0$, i.e. when multiple zero-crossings are present. At the point of incipient loop formation, three real zero-crossings appear due to the odd symmetry of the elastic stress (Fig. 3). For multiple zero-crossings, the slope of the elastic stress $\sigma'(x)$ must change sign from positive, to negative, and back to positive. Therefore self-intersection is equivalent to development of a

region in the center of the elastic stress curve which has negative slope, and which must occur at $x = 0$ to retain odd-symmetry. Therefore, a sufficient quantitative criteria for self-intersection of viscous curves is a negative slope in the decomposed elastic stress at $x = \gamma(t)/\gamma_0 = 0$,

$$\left.\frac{d\sigma'}{dx}\right|_{x=0} < 0 . \tag{5}$$

By analogy, it is possible for the elastic projection of stress $\sigma(t)$ vs. strain $\gamma(t)$ to form secondary loops when sufficient viscous nonlinearity is present. The criteria for self-intersection of elastic projections is

$$\left.\frac{d\sigma''}{dy}\right|_{y=0} < 0 . \tag{6}$$

In dimensional form, the tangent slopes of the stress at these locations (Eqs. (5) and (6)) correspond to viscoelastic material parameters introduced by Ewoldt *et al.* (2008). The minimum-strain elastic modulus G'_M, and the minimum-rate dynamic viscosity η'_M, are given respectively by

$$\begin{aligned} G'_M &\equiv \left.\frac{d\sigma}{d\gamma}\right|_{\gamma=0} = \left.\frac{d\sigma'}{d\gamma}\right|_{\gamma=0} = e_1 - 3e_3 + 5e_5 - 7e_7 + \ldots \\ \eta'_M &\equiv \left.\frac{d\sigma}{d\dot{\gamma}}\right|_{\dot{\gamma}=0} = \left.\frac{d\sigma''}{d\dot{\gamma}}\right|_{\dot{\gamma}=0} = v_1 - 3v_3 + 5v_5 - 7v_7 + \ldots \end{aligned} \tag{7}$$

where $G'_M \equiv G'$ and $\eta'_M \equiv \eta'$ for a linear viscoelastic response, but in general represent the instantaneous elastic modulus and dynamic viscosity in LAOS at the minimum strains and strain-rates. Note that these specific definitions in terms of the local slopes of the *decomposed* stresses are equivalent to the local slopes of the *total* stress, as shown in Eq.(7). Thus, $G'_M < 0$ and $\eta'_M < 0$ are equivalent to Eqs. (5) and (6).

The criterion $G'_M < 0$ can be described geometrically by the 3-D response curve of Fig. 1. Points α and β are labeled in Fig. 1 to identify points at small finite strains $\mp d\gamma$ immediately before and after the strain is instantaneously zero, respectively (see Fig. 1b). Since the strain and strain-rate inputs are related, points α and β also occur just before and just after the maximum positive strain-rate is achieved, $\dot{\gamma}(t) = +\dot{\gamma}_0$ (c.f. Fig. 1c). The geometrical criterion for apparent self-intersection of a 2-D viscous projection ($\sigma(t)$ vs. $\dot{\gamma}(t)$) is that the stress at point β, σ_β, must

be smaller than the stress at point α, σ_α. This is equivalent to the criteria that $\left.\frac{d\sigma}{d\gamma}\right|_{\gamma=0} \equiv G'_M < 0$ (Fig. 1b).

In terms of the higher harmonic coefficients, in order to meet the criterion $G'_M = e_1 - 3e_3 + 5e_5 - ... < 0$, the third-harmonic elastic Chebyshev coefficient, e_3, must be sufficiently large and positive to induce apparent self-intersection of the viscous Lissajous-Bowditch curves,

$$\frac{e_3}{e_1} > \frac{1}{3}\left(1 + 5\frac{e_5}{e_1} - ...\right). \tag{8}$$

For completeness, we note that the corresponding criterion derived from eq. (7b) for self-intersection of the elastic curves would be

$$\frac{v_3}{v_1} > \frac{1}{3}\left(1 + 5\frac{v_5}{e_1} - ...\right). \tag{9}$$

Fig. 2 shows the normalized Chebyshev spectrums for the Giesekus simulation of Fig. 1. Dashed lines are shown at $e_3/e_1 = 1/3$ and $v_3/v_1 = 1/3$ which indicate the leading order criteria for secondary loops to appear in either the viscous or elastic projection, respectively (however we re-emphasize that when expressed in terms of the material parameters G'_M and η'_M the criteria are general and not limited to leading order expressions such as Eqs. (8-9)). The third-harmonic elastic Chebyshev coefficient is sufficiently large and positive, $e_3/e_1 > 1/3$, such that $G'_M < 0$ and secondary loops appear in the viscous Lissajous-Bowditch curves.

The fundamental interpretation is to recognize that secondary loops appearing in viscous projections of the material response correspond to $G'_M < 0$. A negative slope indicates that the material is unloading elastic contributions to the instantaneous stress faster than new deformation is being accumulated (Ewoldt *et al.* (2008)). If we consider the direction in which the space curve in Fig 1 is traversed, then it is clear that from $\gamma = -\gamma_0$ to $\gamma = 0$ the strain-rate $\dot{\gamma}(t)$ monotonically increases from zero to its maximum value. The existence of a local maximum in stress (e.g. Fig. 1b) within this quadrant of the deformation cycle can be interpreted as a viscoelastic stress overshoot. This overshoot is similar to the overshoot in the shear stress which may occur during start-up of steady shear flow. Many systems can show stress overshoot in the

start-up of steady shear (for example the shear-enhanced disentanglement of polymer melts and solutions or the rupture of network structures can show strong stress overshoots), and this behavior is characteristic of significant microstructural change which requires sufficiently large rates of deformation in concert with sufficient amplitude of deformation (Bird *et al.* (1987)).

The Giesekus model exhibits stress overshoots during the inception of steady shear flow (Bird *et al.* (1987)), and also in LAOS as indicated by $G'_M < 0$ and secondary loops (Fig. 1, 3). In LAOS, we observe that a critical strain amplitude is required, e.g. for $\lambda_1\omega = 1$ we first observe $G'_M < 0$ (and secondary loops) at $\gamma_0 = 5.62$ (Fig. 3). Additionally, we observe that a critical shear-rate is required. For lower frequencies, progressively larger strain amplitudes are needed such that $\lambda_1\omega\gamma_0 \gtrsim 10$ (for instance at $\lambda_1\omega = 0.01$ the range of strain amplitude was extended to $\gamma_0 = 1000$ in order to observe $G'_M < 0$ and the formation of secondary loops). The combined criteria of large strain amplitude *and* large strain-rate amplitude are consistent with the typical criteria for stress overshoot in start-up of steady shear (Bird *et al.* (1987)).

An important distinction between LAOS and start-up of steady shear is the periodic reversal of the flow field in LAOS. As we have noted, the oscillatory responses shown here are the steady periodic waveforms, thus any stress overshoot ($G'_M < 0$) must be reversibly achieved. Microstructures which breakdown irreversibly and cannot reform on the time scale of oscillation would not be expected to show stress overshoot and the corresponding secondary loops in steady-state LAOS deformations (although related features may be observed in the transient response). For example, some polypropylene/organoclay nanocomposites show stress overshoot in reverse start-up experiments only for sufficient rest times before reversal (Letwimolnun *et al.* (2007)). Stress overshoots in LAOS would only be expected if the thixotropic restructuring timescale is smaller than the oscillatory deformation timescale. When this is the case, stress overshoot in steady-state LAOS tests may be anticipated. For example, disentangled polymer chains may have sufficient time to re-entangle, or soft glassy systems may find time to re-structure, during flow reversal and display reversible stress overshoot behavior.

To summarize, we have shown that the apparent self-intersection of 2-D Lissajous-Bowditch curves corresponds to sufficiently large and positive values of the third-harmonic components (Eq. 8), or more generally to the criteria $G'_M < 0$ or $\eta'_M < 0$ (Eqs. (5) and (6)). We find that self-intersection of 2-D Lissajous-Bowditch curve projections is most readily interpreted in terms of

the complementary curve, i.e. the self-intersection of viscous projections is caused by a strong elastic nonlinearity. This corresponds to overshoot in the shear stress in the material and is similar to the stress overshoot which occurs during the start-up of steady shear flow. The distinction for LAOS is that the structural change associated with the overshoot must be at least partially reversible on the timescale of the oscillatory deformation. The signature of secondary loops may therefore act as a means of distinguishing various molecular and microstructural systems which show such reversible stress overshoot behavior. Finally, we note that apparent self-intersections and appearance of secondary loops in the elastic Lissajous-Bowditch projections would correspond to pronounced overshoots in the instantaneous dissipative nature of a material (see eq. 7b); for example a rate-dependent transient shear-thickening response. We are unaware of any experimental observations of such phenomena to date but they do not appear to be prohibited in principle.

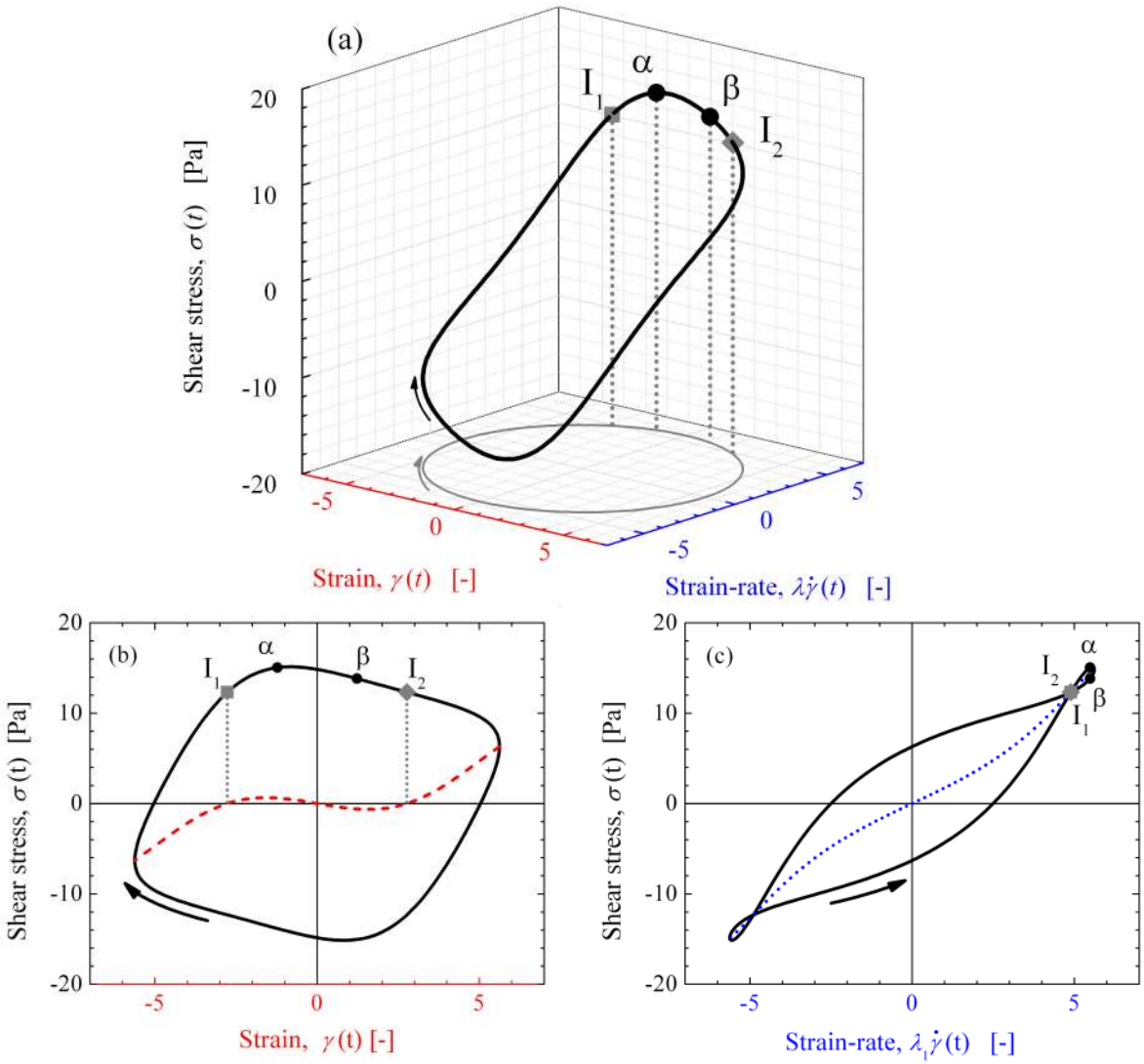

Fig. 1. LAOS simulation of the single-mode Giesekus model, ($\lambda_1\omega = 1$, $\gamma_0 = 5.62$). Only the time-periodic steady state response is shown, with arrows indicating the path trajectory. (a) 3-D Lissajous-Bowditch curve showing the stress response as a function of the orthogonal inputs, $\sigma(\gamma(t),\dot{\gamma}(t))$, (b) 2-D projection onto the plane of stress $\sigma(t)$ and strain $\gamma(t)$, including the instantaneous elastic stress $\sigma'(\gamma(t))$ (dashed line), and (c) 2-D projection onto the plane of stress $\sigma(t)$ and strain-rate $\dot{\gamma}(t)$, including the instantaneous viscous stress $\sigma''(\dot{\gamma}(t))$ (dotted line). The viscous Lissajous-Bowditch curve in (c) shows apparent self-intersection at points I_1 and I_2, although the full space-curve represented in (a) does not intersect at these points.

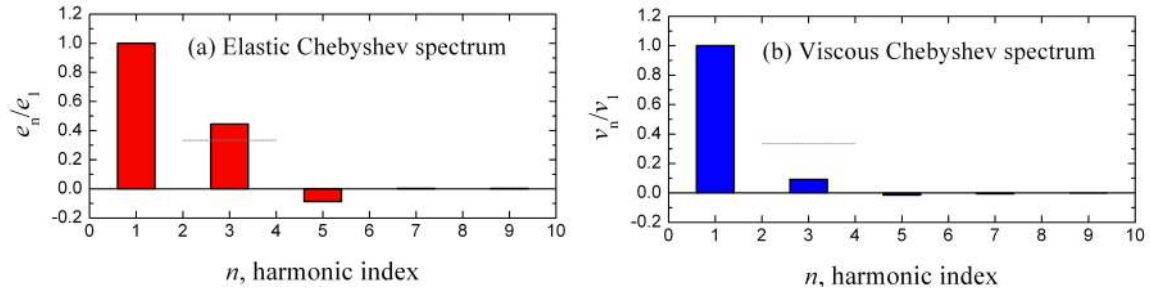

Fig. 2. Single-mode Giesekus model simulation, $\lambda_1\omega = 1$, $\gamma_0 = 5.62$ (a) The elastic Chebyshev spectrum shows that e_3 / e_1 is sufficiently large and positive to create the secondary loops which appear in the viscous Lissajous-Bowditch curve (Fig. 1c). (b) The viscous Chebyshev spectrum. The horizontal dashed lines show the leading-order dimensionless criteria developed in Eqs. (8) and (9) for appearance of secondary loops.

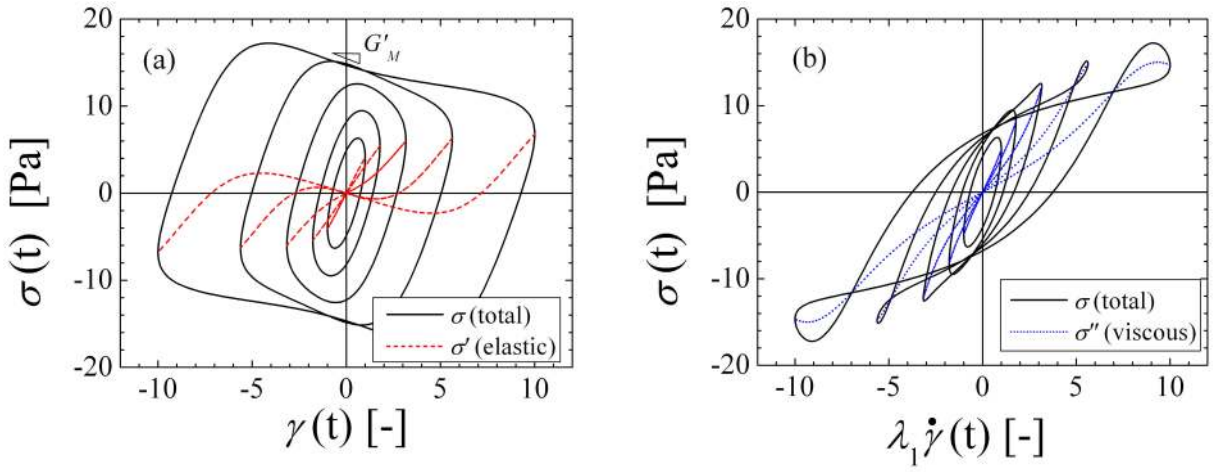

Fig. 3. Incipient secondary loop formation for the single-mode Giesekus model LAOS simulation, $\lambda_1\omega = 1$. (a) The elastic Lissajous-Bowditch projection, in which the criteria $G'_M < 0$ corresponds to the self-intersection and secondary loop formation in (b), the viscous Lissajous-Bowditch projection.

REFERENCES

Bird, R., R. Armstrong and O. Hassager, *Dynamics of polymeric liquids: volume 1 fluid mechanics* (John Wiley & Sons, Inc, New York, 1987)

Burhin, H. G., C. Bailly, R. Keunings, N. Rossion, A. Leygue and H. Pawlowski,"A study of polymer architecture with FT-rheology and large amplitude oscillatory shear (LAOS)," XV International Congress on Rheology: The Society of Rheology 80th Annual Meeting, Monterey (California),The Society of Rheology, **Abstract Booklet,** EM18 (2008)

Cho, K. S., K. H. Ahn and S. J. Lee, "A geometrical interpretation of large amplitude oscillatory shear response," Journal of Rheology **49**(3), 747-758 (2005)

Ewoldt, R. H., A. E. Hosoi and G. H. McKinley, "New measures for characterizing nonlinear viscoelasticity in large amplitude oscillatory shear," Journal of Rheology **52**(6), 1427-1458 (2008)

Giacomin, A. J. and J. M. Dealy (1993). Large-Amplitude Oscillatory Shear, in Techniques in rheological measurement. A. A. Collyer. London, Elsevier Applied Science, Ch. 4

Jeyaseelan, R. S. and A. J. Giacomin, "Network theory for polymer solutions in large amplitude oscillatory shear," Journal of Non-Newtonian Fluid Mechanics **148**(1-3), 24-32 (2008)

Letwimolnun, W., B. Vergnes, G. Ausias and P. J. Carreau, "Stress overshoots of organoclay nanocomposites in transient shear flow," Journal of Non-Newtonian Fluid Mechanics **141**(2-3), 167-179 (2007)

Leygue, A., C. Bailly and R. Keunings, "A tube-based constitutive equation for polydisperse entangled linear polymers," Journal of Non-Newtonian Fluid Mechanics **136**(1), 1-16 (2006)

Rogers, S. A. and D. Vlassopoulos (2009). personal communication.

Stadler, F. J., A. Leygue, H. Burhin and C. Bailly,"The potential of large amplitude oscillatory shear to gain an insight into the long-chain branching structure of polymers," The 235th ACS National Meeting, New Orleans, LA, U.S.A.,Polymer Preprints ACS, **49,** 121-122 (2008)

Tee, T. T. and J. M. Dealy, "Nonlinear viscoelasticity of polymer melts," Transactions of the Society of Rheology **19**(4), 595-615 (1975)

Wilhelm, M., "Fourier-Transform rheology," Macromolecular Materials and Engineering **287**(2), 83-105 (2002)